Crystal structure of N-(4-bromophenyl)-4-[3-(trifluoromethyl)phenyl]-piperazine-1-carbothioamide, $C_{18}H_{17}BrF_3N_3S$

Al-Sanea, Mohammad M ; Blacque, Olivier ; Mohamed, Ahmed A B ; Tiekink, Edward R T ; El-Emam, Ali A

DOI: https://doi.org/10.1515/ncrs-2022-0544

Originally published at:
Al-Sanea, Mohammad M; Blacque, Olivier; Mohamed, Ahmed A B; Tiekink, Edward R T; El-Emam, Ali A (2023).
Crystal structure of N-(4-bromophenyl)-4-[3-(trifluoromethyl)phenyl]-piperazine-1-carbothioamide, $C_{18}H_{17}BrF_3N_3S$.
Zeitschrift für Kristallographie - New Crystal Structures, 238(2):285-288.
DOI: https://doi.org/10.1515/ncrs-2022-0544

Mohammad M. Al-Sanea, Olivier Blacque, Ahmed A. B. Mohamed, Edward R. T. Tiekink and Ali A. El-Emam*

Crystal structure of *N*-(4-bromophenyl)-4-[3-(trifluoromethyl)phenyl]-piperazine-1-carbothioamide, $C_{18}H_{17}BrF_3N_3S$

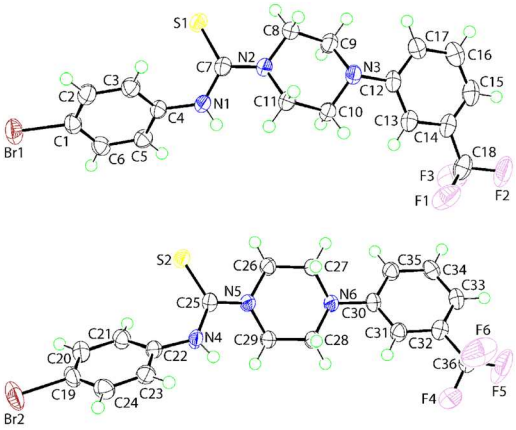

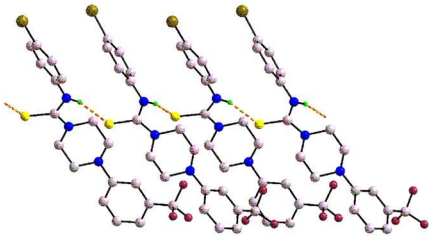

https://doi.org/10.1515/ncrs-2022-0544
Received November 26, 2022; accepted January 3, 2023; published online January 31, 2023

***Corresponding author: Ali A. El-Emam**, Department of Medicinal Chemistry, Faculty of Pharmacy, Mansoura University, Mansoura 35516, Egypt, E-mail: elemam@mans.edu.eg. https://orcid.org/0000-0002-9325-9497
Mohammad M. Al-Sanea, Department of Pharmaceutical Chemistry, College of Pharmacy, Jouf University, Sakaka, Aljouf 72341, Saudi Arabia, E-mail: mmalsanea@ju.edu.sa
Olivier Blacque, Department of Chemistry, University of Zurich, Winterthurerstrasse 190, 8057 Zurich, Switzerland, E-mail: olivier.blacque@chem.uzh.ch
Ahmed A. B. Mohamed, Department of Medicinal Chemistry, Faculty of Pharmacy, Mansoura University, Mansoura 35516, Egypt, E-mail: ahmed_smt@yahoo.com
Edward R. T. Tiekink, Research Centre for Crystalline Materials, School of Medical and Life Sciences, Sunway University, 47500 Bandar Sunway, Selangor Darul Ehsan, Malaysia, E-mail: edwardt@sunway.edu.my. https://orcid.org/0000-0003-1401-1520

Table 1: Data collection and handling.

Crystal:	Colourless plate
Size:	0.22 × 0.03 × 0.02 mm
Wavelength:	Cu *K*α radiation (1.54184 Å)
μ:	4.48 mm^{-1}
Diffractometer, scan mode:	XtaLAB Synergy, ω
θ_{max}, completeness:	74.5°, >99%
$N(hkl)_{measured}$, $N(hkl)_{unique}$, R_{int}:	38,076, 7420, 0.026
Criterion for I_{obs}, $N(hkl)_{gt}$:	$I_{obs} > 2\ \sigma(I_{obs})$, 6960
$N(param)_{refined}$:	477
Programs:	CrysAlis^{PRO} [1], SHELX [2, 3], Olex2 [4]

Abstract

$C_{18}H_{17}BrF_3N_3S$, triclinic, $P\bar{1}$ (no. 2), a = 8.6380(2) Å, b = 14.5082(3) Å, c = 14.8000(3) Å, α = 98.177(2)°, β = 97.015(2)°, γ = 91.111(2)°, V = 1820.89(7) Å^3, Z = 4, $R_{gt}(F)$ = 0.0296, $wR_{ref}(F^2)$ = 0.0783, T = 160 K.

CCDC no.: 2221199

Table 1 contains crystallographic data and Table 2 contains the list of the atoms including atomic coordinates and displacement parameters.

Source of material

4-Bromophenyl isothiocyanate (1.07 g, 0.005 mol) was added to 10 mL of an ethanolic solution of 1-[(3-trifluoromethyl) phenyl]piperazine (1.15 g, 0.005 mol), and the mixture was refluxed for 1 h. The crude product was precipitated upon cooling, followed by filtration, washing with water and drying. Subsequent crystallisation from aqueous ethanol afforded 2.11 g (95%) of (**I**) as colourless plates. Melting point (uncorrected): 441-443 K. **^{1}H NMR** ($CDCl_3$, 500.13 MHz): δ 3.37 (Piperazinyl-H, 4H, t, J = 6.5 Hz), 4.04 (Piperazinyl-H, 4H, t, J = 6.5 Hz), 7.05-7.17 (Aromatic-H & NH, 5H, m), 7.27 (Aromatic-H, 1H, s), 7.39 (Aromatic-H, 1H, t, 1H, J = 10 Hz), 7.48 (Aromatic-H, 2H, d, J = 10 Hz). **^{13}C NMR** ($CDCl_3$, 125.76 MHz): δ 43.15, 43.98 (Piperazinyl-C), 107.38, 111.84, 113.97, 118.09, 120.36, 126.79, 127.11, 127.53, 134.08, 145.65 (Aromatic-C), 125.11 (CF_3),

Table 2: Fractional atomic coordinates and isotropic or equivalent isotropic displacement parameters (Å^2).

Atom	*x*	*y*	*z*	U_{iso}*/U_{eq}
Br1	0.02986 (3)	0.32258 (2)	0.12114 (2)	0.03529 (7)
S1	0.20919 (5)	0.13799 (3)	0.52076 (3)	0.02374 (10)
F1	1.31551 (16)	0.22694 (12)	0.78143 (10)	0.0506 (4)
F2	1.39456 (18)	0.19727 (13)	0.91713 (14)	0.0662 (5)
F3	1.25805 (19)	0.31559 (10)	0.89827 (11)	0.0516 (4)
N1	0.44623 (19)	0.19903 (12)	0.44082 (12)	0.0245 (3)
H1	0.531 (3)	0.2284 (19)	0.4534 (19)	0.036 (7)*
N2	0.51512 (18)	0.12134 (11)	0.56345 (11)	0.0217 (3)
N3	0.76185 (18)	0.09660 (11)	0.70631 (11)	0.0236 (3)
C1	0.1632 (2)	0.28321 (14)	0.21907 (13)	0.0253 (4)
C2	0.1534 (2)	0.19098 (15)	0.23319 (14)	0.0270 (4)
H2	0.083563	0.147744	0.193001	0.032*
C3	0.2469 (2)	0.16222 (14)	0.30690 (14)	0.0254 (4)
H3	0.242293	0.098967	0.316686	0.030*
C4	0.3467 (2)	0.22645 (13)	0.36599 (13)	0.0216 (4)
C5	0.3587 (2)	0.31805 (13)	0.34923 (14)	0.0239 (4)
H5	0.430063	0.361156	0.388483	0.029*
C6	0.2667 (2)	0.34690 (14)	0.27516 (14)	0.0251 (4)
H6	0.274896	0.409374	0.263372	0.030*
C7	0.3999 (2)	0.15322 (12)	0.50757 (13)	0.0204 (4)
C8	0.4848 (2)	0.07597 (14)	0.64187 (14)	0.0260 (4)
H8A	0.493807	0.007768	0.626455	0.031*
H8B	0.377357	0.088163	0.655959	0.031*
C9	0.6007 (2)	0.11258 (15)	0.72519 (14)	0.0277 (4)
H9A	0.587521	0.180182	0.742420	0.033*
H9B	0.579634	0.081014	0.777735	0.033*
C10	0.7940 (2)	0.14197 (14)	0.62798 (13)	0.0237 (4)
H10A	0.900683	0.127762	0.613530	0.028*
H10B	0.789288	0.210336	0.644413	0.028*
C11	0.6771 (2)	0.10914 (13)	0.54384 (13)	0.0227 (4)
H11A	0.696480	0.144702	0.493735	0.027*
H11B	0.691949	0.042463	0.522447	0.027*
C12	0.8746 (2)	0.11135 (13)	0.78500 (14)	0.0252 (4)
C13	1.0182 (2)	0.15724 (13)	0.78545 (14)	0.0251 (4)
H13	1.042415	0.180323	0.731690	0.030*
C14	1.1261 (2)	0.16924 (14)	0.86450 (15)	0.0277 (4)
C15	1.0961 (3)	0.13708 (17)	0.94423 (16)	0.0373 (5)
H15	1.171003	0.145448	0.997603	0.045*
C16	0.9527 (3)	0.0921 (2)	0.94383 (18)	0.0455 (6)
H16	0.928431	0.070452	0.998241	0.055*
C17	0.8449 (3)	0.07832 (17)	0.86598 (17)	0.0374 (5)
H17	0.748800	0.045849	0.867223	0.045*
C18	1.2730 (3)	0.22557 (16)	0.86574 (16)	0.0339 (5)
Br2	−0.44430 (3)	0.06290 (2)	0.10760 (2)	0.04414 (8)
S2	−0.28605 (5)	0.36486 (3)	0.52555 (3)	0.02317 (10)
F4	0.81934 (17)	0.34564 (12)	0.79008 (10)	0.0499 (4)
F5	0.90840 (19)	0.42944 (12)	0.91585 (15)	0.0702 (6)
F6	0.7446 (2)	0.31742 (13)	0.91454 (14)	0.0663 (5)
N4	−0.05632 (19)	0.27716 (11)	0.44524 (12)	0.0235 (3)
H4	0.030 (3)	0.2506 (18)	0.4569 (18)	0.033 (7)*
N5	0.02240 (18)	0.39313 (11)	0.56546 (11)	0.0217 (3)
N6	0.27815 (18)	0.46454 (11)	0.70017 (11)	0.0221 (3)
C19	−0.3261 (2)	0.12955 (14)	0.21486 (14)	0.0269 (4)
C20	−0.3463 (2)	0.22411 (14)	0.23598 (14)	0.0270 (4)
H20	−0.419724	0.254532	0.198283	0.032*
C21	−0.2585 (2)	0.27427 (14)	0.31277 (14)	0.0249 (4)
H21	−0.268984	0.339641	0.326756	0.030*
C22	−0.1551 (2)	0.22833 (13)	0.36913 (13)	0.0212 (4)
C23	−0.1372 (2)	0.13288 (13)	0.34686 (14)	0.0245 (4)
H23	−0.066301	0.101693	0.385320	0.029*
C24	−0.2220 (2)	0.08300 (14)	0.26898 (15)	0.0283 (4)
H24	−0.208802	0.018089	0.253200	0.034*
C25	−0.0975 (2)	0.34492 (12)	0.51099 (13)	0.0200 (4)
C26	−0.0018 (2)	0.46232 (13)	0.64427 (14)	0.0248 (4)
H26A	−0.107314	0.452448	0.661682	0.030*
H26B	0.005411	0.525714	0.627319	0.030*
C27	0.1203 (2)	0.45378 (14)	0.72517 (13)	0.0246 (4)
H27A	0.105376	0.502209	0.777355	0.030*
H27B	0.107393	0.392068	0.745092	0.030*
C28	0.3026 (2)	0.39209 (13)	0.62448 (13)	0.0237 (4)
H28A	0.292659	0.329932	0.643910	0.028*
H28B	0.409020	0.399730	0.607522	0.028*
C29	0.1825 (2)	0.39919 (14)	0.54223 (13)	0.0231 (4)
H29A	0.199566	0.459187	0.519707	0.028*
H29B	0.196463	0.348320	0.492042	0.028*
C30	0.3984 (2)	0.48190 (13)	0.77514 (13)	0.0217 (4)
C31	0.5299 (2)	0.42774 (13)	0.78379 (13)	0.0234 (4)
H31	0.540025	0.375087	0.739046	0.028*
C32	0.6461 (2)	0.45088 (14)	0.85792 (14)	0.0246 (4)
C33	0.6372 (2)	0.52789 (14)	0.92368 (14)	0.0272 (4)
H33	0.718308	0.543501	0.973317	0.033*
C34	0.5063 (2)	0.58188 (14)	0.91513 (14)	0.0272 (4)
H34	0.497665	0.634978	0.959630	0.033*
C35	0.3884 (2)	0.55925 (13)	0.84271 (13)	0.0246 (4)
H35	0.299416	0.596584	0.838610	0.029*
C36	0.7791 (3)	0.38692 (15)	0.87015 (15)	0.0312 (4)

178.50 (C=S). Analysis calculated for $C_{18}H_{17}BrF_3N_3S$: C, 48.66; H, 3.86; N, 9.46; S, 7.22%. Found: C, 46.50; H, 3.90; N, 9.44; S, 7.20%.

Experimental details

The C-bound H atoms were geometrically placed (C–H = 0.95–0.99 Å) and refined as riding with U_{iso}(H) = 1.2U_{eq}(C). The N-bound H atoms were located in a difference map and refined freely.

Comment

The investigation of the title compound (**I**) was performed within the framework of medicinal chemistry. Thus, the piperazine-1-carbothioamide residue of (**I**) has been identified

as a core pharmacophore in anti-fungal [5], anti-bacterial [6, 7], anti-inflammatory [8] and neuroprotective agents [9]. Herein, description of the synthesis, crystallographic characterisation as well as analysis of the calculated Hirshfeld surface are provided.

The molecular structures of the two independent molecules comprising the asymmetric-unit of **(I)** are shown in the upper images of the figure (70% probability ellipsoids). The molecules exhibit very similar conformations. Thus, the central CN_2S residue for the S1-containing molecule has a r.m.s. deviation of 0.0021 Å and forms dihedral angles of 58.87(7) and 30.03(9)° with the bromophenyl and trifluorophenyl rings, respectively; the dihedral angle between the substituted phenyl rings is 48.22(8)°. The equivalent values for the second independent molecule are close, at 0.0062 Å and 53.9(7), 29.08(9) and 27.54(9)°, respectively, indicating the molecular conformations differ primarily only in the relative dispositions of the pendant phenyl groups.

Within the CN_2S chromophore, the C7–N1, N2 bond lengths are experimentally equivalent [1.361(3) & 1.347(2) Å] and significantly shorter, as expected, than the C4–N1 [1.425(2) Å], and C8–N2 [1.461(2) Å] and C11–N2 [1.472(2) Å] bond lengths. The equivalent values for the second independent molecule are 1.366(2), 1.349(2), 1.419(2), 1.465(2) and 1.470(2) Å, indicating a close match with the first independent molecule.

There are three closely related literature structures with a piperazine linked to a CN_2S chromophore. Two of these have a phenyl group at the N3-position, and at the N1-position, an adamantan-1-yl group [10] or a fused, three-ring system [11]. The third precedent has a 2-trifluoromethylphenyl group at the N3-position and an ethyl group at the N1-position [12]. The key geometric parameters among the four structures are in close accord.

The anti-disposition of the thione–S and amide–H atoms facilitates the formation of amide–N–H···S(thione) hydrogen bonds [N1–H1···$S2^{i}$: H1···$S2^{i}$ = 2.53(3) Å, N1···$S2^{i}$ = 3.3055(18) Å with angle at H1 = 156(2)° and N4–H4···S1: H4···S1 = 2.48(3) Å, N4···S1 = 3.2835(17) Å with angle at N2 = 157(2)° for symmetry operation (i): 1 + *x*, *y*, *z*] within a zigzag chain of alternate independent molecules aligned along the a-axis, as illustrated in the lower view of the figure (non-participating H atoms have been removed for clarity). The independent molecules self-associate *via* methylene–C–H···S(thione) [C11–H11b···$S1^{ii}$: H11b···$S1^{ii}$ = 2.78 Å, C11···$S1^{ii}$ = 3.7583(19) Å with angle at H11b = 169° and C29–H29a···$S2^{iii}$: H29a···$S2^{iii}$ = 2.84 Å, C29···$S2^{iii}$ = 3.821(2) Å with angle at H29a = 172° for (ii): 1 – *x*, –*y*, 1 – *z* and (iii): –*x*, 1 – *y*, 1 – *z*] interactions within a supramolecular layer in the ab-plane. The layers stack along the c-axis with close, Br2···$Br2^{iv}$ contacts between centrosymmetrically related molecules. Thus, Br2···$Br2^{iv}$ = 3.4541(4) Å with an angle at Br2 = 163.76(6)° for (iv): –1 – x, –y, –z; the sum of the van der Waals radii amounts to 3.70 Å [13].

An analysis of the calculated Hirshfeld surfaces was also conducted to comprehend further the molecular packing and to ascertain differences in the surface contacts exhibited by the independent molecules [14, 15]. The surface contacts for each independent molecule are dominated by contacts involving H, i.e. H···H 87.7% for the S1-containing molecule [87.3% for the S2-containing molecule]. The major contributors to the surface contacts are H···H 29.9% [27.6%], C···H/H···C 17.6% [18.1%], F···H/H···F 16.1% [19.5%], S···H/H···S 10.9% [11.2%], Br···H/H···Br 10.0% [8.3%] and N···H/H···N 3.2% [2.6%]. The differential in the F···H/H···F contacts is the greatest distingushing feature between the molecules. Another notable difference relates to Br···Br contacts which are 0.0 and 1.3% for the independent molecules, respectively. There are Br···F/F···Br contacts worth highlighting, namely 4.6 and 3.4%, respectively, as well as F···F contacts of 1.4 and 2.3%, respectively.

Author contributions: All the authors have accepted responsibility for the entire content of this submitted manuscript and approved submission.

Research funding: This work was funded by the Deanship of Scientific Research at Jouf University under grant No. DSR-2021-01-03115.

Conflict of interest statement: The authors declare no conflicts of interest regarding this article.

References

1. Rigaku Oxford Diffraction. CrysAlis^{PRO}; Rigaku Corporation: Oxford, UK, 2021.
2. Sheldrick G. M. A short history of SHELX. *Acta Crystallogr.* 2008, *A64*, 112–122.
3. Sheldrick G. M. Crystal structure refinement with SHELXL. *Acta Crystallogr.* 2015, *C71*, 3–8.
4. Dolomanov O. V., Bourhis L. J., Gildea R. J., Howard J. A. K., Puschmann H. OLEX2: a complete structure solution, refinement and analysis program. *J. Appl. Crystallogr.* 2009, *42*, 339–341.
5. Bala V., Mandalapu D., Gupta S., Jangir S., Kushwaha B., Chhonker Y. S., Chandasana H., Krishna S., Rawat K., Krishna A., Singh M., Sankhwar S. N., Shukla P. K., Maikhuri J. P., Bhatta R. S., Siddiqi M. I., Tripathi R., Gupta G., Sharma V. L. *N*-Alkyl/aryl-4-(3-substituted-3-phenylpropyl)piperazine-1-carbothioamide as dual-action vaginal microbicides with reverse transcriptase inhibition. *Eur. J. Med. Chem.* 2015, *101*, 640–650.
6. Foley T. L., Rai G., Yasgar A., Daniel T., Baker H. L., Attene-Ramos M., Kosa N. M., Leister W., Burkart M. D., Jadhav A., Simeonov A.,

Maloney D. J. 4-(3-Chloro-5-(trifluoromethyl)pyridin-2-yl)-*N*-(4-methoxypyridin-2-yl)piperazine-1-carbothioamide (ML267), a potent inhibitor of bacterial phosphopantetheinyl transferase that attenuates secondary metabolism and thwarts bacterial growth. *J. Med. Chem.* 2014, *57*, 1063–1078.

7. Konno S., Ishikawa F., Suzuki T., Dohmae N., Kakeya H., Tanabe G. A. Chemoproteomics approach to investigate phosphopantetheine transferase activity at the cellular level. *ChemBioChem* 2017, *18*, 1855–1862.
8. Karthik C. S., Manukumar H. M., Sandeep S., Sudarshan B. L., Nagashree S., Mallesha L., Rakesh K. P., Sanjay K. R., Mallu P., Qin H. L. Development of piperazine-1-carbothioamide chitosan silver nanoparticles (P1C–Tit*CAgNPs) as a promising anti-inflammatory candidate: a molecular docking validation. *MedChemComm* 2018, *9*, 713–724.
9. Agrawal S., Kumari R., Sophronea T., Kumari N., Luthra P. M. Design and synthesis of benzo[*d*]thiazol-2-yl-methyl-4-(substituted)-piperazine-1-carbothioamide as novel neuronal nitric oxide inhibitors and evaluation of their neuroprotecting effect in 6-OHDA-induced unilateral lesioned rat model of Parkinson's disease. *Biomed. Pharmacother.* 2022, *156*, 113838.
10. Al-Abdullah E. S., Ghabbour H. A., Alkahtani H. M., Al-Tamimi A.-M. S., El-Emam A. A. Crystal structure of *N*-(adamantan-1-yl)-4-phenylpiperazine-1-carbothioamide, $C_{21}H_{29}N_3S$. *Z. Kristallogr. N. Cryst. Struct.* 2016, *231*, 991–993.
11. Mishra K. B., Rajkhowa S., Tiwari V. K. An expeditious one-pot synthesis of thiourea derivatives of carbohydrates from sugar azides. *J. Carbohydr. Chem.* 2020, *29*, 334–353.
12. Al-Wahaibi L. H., Blacque O., Al-Shaalan N. H., Tiekink E. R. T., El-Emam A. A. Crystal structure of *N*-ethyl-4-(3-(trifluoromethyl)phenyl)piperazine-1-carbothioamide, $C_{14}H_{18}F_3N_3S$. *Z. Kristallogr. N. Cryst. Struct.* 2023, *268*, 45–47.
13. Spek A. L. *checkCIF* validation ALERTS: what they mean and how to respond. *Acta Crystallogr.* 2020, *E76*, 1–11.
14. Spackman P. R., Turner M. J., McKinnon J. J., Wolff S. K., Grimwood D. J., Jayatilaka D., Spackman M. A. CrystalExplorer: a program for Hirshfeld surface analysis, visualization and quantitative analysis of molecular crystals. *J. Appl. Crystallogr.* 2021, *54*, 1006–1011.
15. Tan S. L., Jotani M. M., Tiekink E. R. T. Utilizing Hirshfeld surface calculations, non-covalent interaction (NCI) plots and the calculation of interaction energies in the analysis of molecular packing. *Acta Crystallogr.* 2019, *E75*, 308–318.